Nonlinear Dyn
https://doi.org/10.1007/s11071-023-08498-4

ORIGINAL PAPER

A minimal model for adaptive SIS epidemics

Massimo A. Achterberg · Mattia Sensi

Received: 3 November 2022 / Accepted: 11 April 2023

Abstract The interplay between disease spreading and personal risk perception is of key importance for modelling the spread of infectious diseases. We propose a planar system of ordinary differential equations (ODEs) to describe the co-evolution of a spreading phenomenon and the average link density in the personal contact network. Contrary to standard epidemic models, we assume that the contact network changes based on the current prevalence of the disease in the population, i.e. the network adapts to the current state of the epidemic. We assume that personal risk perception is described using two functional responses: one for link-breaking and one for link-creation. The focus is on applying the model to epidemics, but we also highlight other possible fields of application. We derive an explicit form for the basic reproduction number and guarantee the existence of at least one endemic equilibrium, for all possible functional responses. Moreover, we show that for all functional responses, limit cycles do not exist. This means that our minimal model is not able to reproduce consequent waves of an epidemic, and more complex disease or behavioural dynamics are required to reproduce epidemic waves.

Keywords Network epidemiology · Planar system · Risk perception · SIS epidemics · Adaptive networks

1 Introduction

Classical compartmental models in epidemiology rely on the widely accepted assumption of homogeneous mixing. Homogeneous mixing implies that any individual in a population has the same probability of meeting every other individual, regardless of their location, activities or age. While this assumption greatly simplifies the analysis of such models, its interpretation clashes with the reality of human interaction, which is known to be heterogeneous and exhibits community structure [1]. Network models have been proposed and studied to include a more realistic pattern of connections between individuals [2].

Most network-based research focuses on contact patterns that remain fixed over time. However, real-world contacts vary over time, especially during epidemic outbreaks, because of individual decisions of people to avoid contact with other people. Such networks are called *adaptive* networks, because the network adapts itself to the spread of the disease [3].

The excellent review by Verelst et al. [4] provides an overview of various practical approaches for the mathematical modelling of the interplay between dis-

M. A. Achterberg (✉)
Faculty of Electrical Engineering, Mathematics and Computer Science, Delft University of Technology, P.O. Box 5031, 2600 GA Delft, The Netherlands
e-mail: M.A.Achterberg@tudelft.nl

M. Sensi (✉)
MathNeuro Team, Inria at Université Côte d'Azur, 2004 Rte des Lucioles , 06410 Biot, France
e-mail: mattia.sensi@inria.fr

Published online: 06 May 2023

ease and human behavior. A multi-layer approach was adopted by Sahneh et al. [5], where one layer describes the disease transmission and another layer the awareness of individuals about the disease. Gross et al. [6] proposed a rewiring mechanism, which rewires the link between two connected susceptible-infected nodes to two susceptible nodes. Kiss et al. [7] (and independently Achterberg et al. [8]) introduced a Link Activation-Deactivation model, in which links can be broken or created between any two nodes, where the rate to break or create a link depends on the health state of the two nodes attached to that link. Jolad et al. [9] assumes that all individuals have a preferred number of neighbours, subject to random link addition and removals. The preferred degree is taken to be a function of the current number of infected nodes in the network. Brauer [10] discusses an SIR model in which a certain percentage of the links is removed. The removal percentage is larger if the link is connected to infected nodes rather than susceptible nodes. All abovementioned models capture a particular aspect of human behavior on disease dynamics, but most are so complicated that an exact analysis is completely infeasible. The reason is that the models often involve a large amount of individuals or equations, or the infection probabilities involve the computation of many dependent random variables.

In this work, we propose a minimal model consisting of two ODEs, one for the viral prevalence (i.e. the fraction of individuals currently carrying the disease) in the population using the NIMFA equations [11], and one for the link density of the contact network. Our model is minimal in terms of the number of equations and parameters, while still capturing key aspects of behavioural disease dynamics. We model the creation and removal of edges as an overall increase or decrease of the link density of the contact network. We call the model adaptive NIMFA (aNIMFA), in line with earlier work [12]. The core aspect of aNIMFA are the *functional responses* of individuals to create or break links in the network, based on the current number of infected people. In predator–prey systems like Volterra-Lotka dynamics, Holling introduced functional responses to describe the food intake by predators as a function of the number of available prey [13]. A preliminary analysis of the aNIMFA model was performed by Achterberg and Van Mieghem [12], but only for specific functional responses. We extend the results from [12] by considering general functional responses and by providing a more detailed analysis.

The aNIMFA model is not limited to modelling epidemic spread, but can be utilised for describing general spreading phenomena, including opinion dynamics, Maki-Thompson rumour spread, innovation spread and epileptic seizures in the human brain. If the dynamics evolve over a network structure and the link density can be modelled by link-breaking and link-creation dynamics, the aNIMFA model can be generalised to such models. In the context of epidemics, one would expect the removal (resp. creation) of links to be directly (resp. inversely) proportional to the prevalence. For other spreading phenomena, such as rumor spreading, this might not be the case, and other choices for the functional responses can be made. The simplicity of the aNIMFA model makes it a promising tool for future generalizations and for the integration of more complex mechanisms.

Lastly, we consider the situation where the network changes slowly compared to the spread of the disease, and we study the qualitative behaviour of the resulting model using Geometric Singular Perturbation Theory (GSPT) [14,15]. Techniques from GSPT have been applied to epidemiological models in which the loss of immunity and demography are slow compared to infection and recovery from a disease in [16,17]. Additionally, similar techniques were applied to epidemics modelling e.g. in [18–22].

The paper is structured as follows. We introduce the aNIMFA model in Sect. 2 and provide a thorough analysis in Sect. 3. Then we consider several examples of functional responses in Sect. 4. We study a slowly evolving network in Sect. 5 using Geometric Singular Perturbation Theory and present a conclusion in Sect. 6.

2 The aNIMFA model

Consider a well-mixed population of N individuals, subject to the spread of a disease. Of primary importance is the *prevalence* $y(t)$, which is the average fraction of infected individuals at time t. The governing equation for the prevalence y of the SIS process for a well-mixed population is given by

$$\frac{\mathrm{d}y}{\mathrm{d}t} = -\delta y + \beta y(1-y)z, \tag{1}$$

where the curing process is denoted by its rate δ, the infection process by the corresponding rate β and z is

the link density of the contact network, i.e. the average fraction of connections between all individuals compared to the total amount of possible connections. In the classical model, the link density z is not varying over time. In the first term on the right-hand side of Eq. (1), the prevalence decreases proportional to the current number of infected cases. The second term on the right-hand side in Eq. (1) increases the prevalence because of contact between infected y and susceptible $1-y$ nodes. Because of the homogeneous mixing, we multiply with the link density z to obtain the average number of contacts. Equation (1) is also equivalent to the N-Intertwined Mean-Field Approximation (NIMFA) of a Markovian SIS process on a complete static graph with link weights z, equal initial conditions for all nodes and homogeneous infection and curing rates [11].

Contrary to the static SIS process, we assume that the link density $z(t)$ is varying over time and its dynamics is governed by a link-breaking and a link-creation process. Then the link density $z(t)$ changes over time as

$$\frac{\mathrm{d}z}{\mathrm{d}t} = -\zeta z f_{\mathrm{br}}(y) + \xi(1-z) f_{\mathrm{cr}}(y), \tag{2}$$

where ζ is the link-breaking rate, ξ the link-creation rate and $f_{\mathrm{br}}(y)$ and $f_{\mathrm{cr}}(y)$ are the functional responses to the link-breaking and link-creation process, respectively. The breaking (resp. creation) of links translates into decreasing (increasing) the link density z in Eq. (2), implying that f_{br} and f_{cr} must be non-negative. We assume the parameters δ, β, ζ, ξ to be $\mathcal{O}(1)$ and positive. The link density z has been normalised, such that $z=1$ is the maximum link density (corresponding to a complete graph) and $z=0$ corresponds to an empty graph (no connections, so the link density is zero).

Equations (1) and (2) can be simplified by introducing the scaled time $\tilde{t} = \delta t$. We additionally introduce the *effective infection rate* $\tau = \beta/\delta$. Using the transformations $\tilde{\zeta} = \zeta/\delta$ and $\tilde{\xi} = \xi/\delta$, the well-mixed adaptive NIMFA (aNIMFA) equations are obtained (after dropping the tildes, for ease of notation)

$$\frac{\mathrm{d}y}{\mathrm{d}t} = -y + \tau y(1-y)z, \tag{3a}$$

$$\frac{\mathrm{d}z}{\mathrm{d}t} = -\zeta z f_{\mathrm{br}}(y) + \xi(1-z) f_{\mathrm{cr}}(y), \tag{3b}$$

feasible region $0 \le y \le 1, 0 \le z \le 1$.

We introduce, for ease of notation, the *effective link-breaking rate* $\omega = \zeta/\xi$; this will be useful in Sect. 3.2. The initial conditions $y(0) \in [0,1]$ and $z(0) \in [0,1]$ describe the initial prevalence and link-density, respectively. We assume that the functional responses $f_{\mathrm{br}}(y)$ and $f_{\mathrm{cr}}(y)$ are non-negative, sufficiently regular functions on the interval $0 \le y \le 1$. We exclude the possibility that $f_{\mathrm{br}}(y) = 0$ and $f_{\mathrm{cr}}(y) = 0$ for all y, as in this case, the link density z is not affected by f_{br} and f_{cr} and remains constant over time.

3 Analysis of the model

Prior to confining ourselves to specific link-breaking and link-creation functions f_{br} and f_{cr}, we first derive general results for the aNIMFA model.

Lemma 1 *Consider a solution of system (3) starting at* $(y(0), z(0)) \in [0,1]^2$. *Recall that* $f_{\mathrm{br}}(y), f_{\mathrm{cr}}(y) \ge 0$ *for all* $y \in [0,1]$. *Then,* $(y(t), z(t)) \in [0,1]^2$ *for all* $t \ge 0$, *meaning* $[0,1]^2$ *is forward invariant for system (3).*

Proof We calculate

$$\left.\frac{\mathrm{d}y}{\mathrm{d}t}\right|_{y=0} = 0, \quad \left.\frac{\mathrm{d}y}{\mathrm{d}t}\right|_{y=1} = -1 < 0,$$

$$\left.\frac{\mathrm{d}z}{\mathrm{d}t}\right|_{z=0} = \xi f_{\mathrm{cr}}(y) \ge 0, \quad \left.\frac{\mathrm{d}z}{\mathrm{d}t}\right|_{z=1} = -\zeta f_{\mathrm{br}}(y) \le 0,$$

which proves the forward invariance of $[0,1]^2$. □

3.1 Disease-free equilibrium

The aNIMFA model always has one steady state $y_0 = 0$, which corresponds to the situation in which no infected individuals are present in the population. In line with the literature, we call this steady state the *disease-free equilibrium* (DFE). The DFE of the mean-field equations (3) equals

$$y_0 = 0,$$

$$z_0 = \begin{cases} \frac{f_{\mathrm{cr}}(0)}{\omega f_{\mathrm{br}}(0) + f_{\mathrm{cr}}(0)} & \text{if } f_{\mathrm{br}}(0) \neq 0 \text{ or } f_{\mathrm{cr}}(0) \neq 0, \\ c & \text{if } f_{\mathrm{br}}(0) = f_{\mathrm{cr}}(0) = 0, \end{cases}$$

for any $c \in [0,1]$.

3.2 Endemic equilibria

Depending on the choice of the functional responses f_{br} and f_{cr}, multiple additional steady states may exist, which are called the *endemic equilibria* (EE). Recall that $\omega = \zeta/\xi$ is the effective link-breaking rate of system (3). The endemic equilibria are the solutions of the generally non-linear equation

$$\omega f_{\mathrm{br}}(y_{\mathrm{E}}) = (\tau - 1) f_{\mathrm{cr}}(y_{\mathrm{E}}) - \tau y_{\mathrm{E}} f_{\mathrm{cr}}(y_{\mathrm{E}}), \tag{4}$$

and the corresponding steady-state link density z_{E} follows as

$$z_{\mathrm{E}} = \frac{1}{\tau(1 - y_{\mathrm{E}})}. \tag{5}$$

We remark that the solution $y_{\mathrm{E}} = 1$ is never a valid EE for any functional responses f_{br} and f_{cr}, which follows immediately from substituting $y_{\mathrm{E}} = 1$ into Eq. (4). Hence, if an EE exist, the steady-state prevalence y_{E} must be in the open interval $(0, 1)$. We further investigate the existence of endemic equilibria in Sect. 3.4.

3.3 Linear stability analysis

We analyse the linear stability of the steady states by computing the Jacobian of Eq. (3) as

$$J = \begin{pmatrix} -1 + \tau(1 - 2y_{\mathrm{E}})z_{\mathrm{E}} & \tau y_{\mathrm{E}}(1 - y_{\mathrm{E}}) \\ -\zeta z_{\mathrm{E}} f'_{\mathrm{br}}(y_{\mathrm{E}}) + \xi(1 - z_{\mathrm{E}}) f'_{\mathrm{cr}}(y_{\mathrm{E}}) & -\zeta f_{\mathrm{br}}(y_{\mathrm{E}}) - \xi f_{\mathrm{cr}}(y_{\mathrm{E}}) \end{pmatrix}. \tag{6}$$

Evaluating (6) in the disease-free equilibrium $y_{\mathrm{E}} = 0$, $z_{\mathrm{E}} = z_0$, we find

$$J(0, z_0) = \begin{pmatrix} -1 + \tau z_0 & 0 \\ -\zeta z_0 f'_{\mathrm{br}}(0) + \xi(1 - z_0) f'_{\mathrm{cr}}(0) & -\zeta f_{\mathrm{br}}(0) - \xi f_{\mathrm{cr}}(0) \end{pmatrix}. \tag{7}$$

Since the Jacobian for the disease-free equilibrium is lower-triangular, the eigenvalues are $\lambda_1 = -1 + \tau z_0$ and $\lambda_2 = -\zeta f_{\mathrm{br}}(0) - \xi f_{\mathrm{cr}}(0)$. The eigenvalues are always real, so (un)stable spirals cannot be observed. We now consider several cases.

1. **Case** $f_{\mathrm{br}}(0) = 0$ and $f_{\mathrm{cr}}(0) = 0$
   The eigenvalues are $\lambda_1 = -1 + \tau z_0$ and $\lambda_2 = 0$, which makes the stability undeterminable using linear stability analysis.
2. **Case** $f_{\mathrm{br}}(0) = 0$ and $f_{\mathrm{cr}}(0) > 0$
   The eigenvalues are $\lambda_1 = -1 + \tau$ and $\lambda_2 = -\xi f_{\mathrm{cr}}(0)$. Thus the disease-free equilibrium is a stable node if $\tau < 1$ and an unstable node if $\tau > 1$. For $\tau = 1$, the stability is undetermined. In this case, $z_0 = 1$.
3. **Case** $f_{\mathrm{br}}(0) > 0$ and $f_{\mathrm{cr}}(0) = 0$
   The eigenvalues are $\lambda_1 = -1$ and $\lambda_2 = -\zeta f_{\mathrm{br}}(0)$, thus the DFE is a stable node. In this case, $z_0 = 0$.
4. **Case** $f_{\mathrm{br}}(0) > 0$ and $f_{\mathrm{cr}}(0) > 0$
   The eigenvalues are $\lambda_1 = -1 + \tau \frac{f_{\mathrm{cr}}(0)}{\omega f_{\mathrm{br}}(0) + f_{\mathrm{cr}}(0)}$ and $\lambda_2 = -\zeta f_{\mathrm{br}}(0) - \xi f_{\mathrm{cr}}(0)$. Eigenvalue $\lambda_2 < 0$, thus the stability solely depends on λ_1. The disease-free equilibrium is a stable node if $\tau < \frac{\omega f_{\mathrm{br}}(0) + f_{\mathrm{cr}}(0)}{f_{\mathrm{cr}}(0)}$, an unstable node if $\tau > \frac{\omega f_{\mathrm{br}}(0) + f_{\mathrm{cr}}(0)}{f_{\mathrm{cr}}(0)}$ and is undetermined otherwise.

We remark that, in cases 2 and 4, the linear stability or instability of the DFE coincides with R_0 derived in Sect. 3.4 being smaller or bigger than 1.

Unfortunately, we cannot directly analyse the stability of the endemic equilibria, because (i) we do not know y_{E} nor z_{E} and (ii) we require the functions f_{br} and f_{cr} and its derivatives f'_{br} and f'_{cr} to determine the stability. Moreover, the existence of multiple endemic equilibria rules out the possibility of finding a Lyapunov function to prove the global stability of system (3). Nevertheless, for specific functional responses f_{br} and f_{cr} that have only a single EE, one could attempt to construct a Lyapunov function, which is outside the scope of this paper.

3.4 Basic reproduction number

In this section, we provide an expression for the *basic reproduction number* R_0, also known as the epidemic threshold, which is the number of secondary infections produced by one average infected individual in an otherwise susceptible population. At the point $R_0 = 1$, the disease-free equilibrium loses stability and an endemic equilibrium emerges. We compute the basic reproduction number R_0 using the next generation matrix method, which was first introduced in [23], then generalized in [24] (see also [25]). Even though the compartmental component of system (3) is one-dimensional (the equation for the link density z does not count) and the analysis could also be done by local stability analysis, we have chosen for the next generation matrix method due to its widely spread use.

We rewrite the first entry of (7) as $J_{11} = M_{11} - V_{11}$, with $M_{11}, V_{11} > 0$. The only such splitting possible,

assuming $f_{\rm cr}(0) > 0$, is

$$M_{11} = \tau z_0, \quad V_{11} = 1.$$

Then, the basic reproduction number R_0 is $M_{11}V_{11}^{-1}$, i.e.

$$R_0 = \tau \frac{f_{\rm cr}(0)}{\omega f_{\rm br}(0) + f_{\rm cr}(0)}. \tag{8}$$

For the case $f_{\rm cr}(0) = 0$, the method does not apply: this models a particularly degenerate situation in our model, as absence of the disease does not increase the connectivity strength. We use this definition of R_0 to prove the following theorem.

Theorem 2 *If $R_0 > 1$, system (3) admits at least one endemic equilibrium.*

Proof It follows from the second equation of system (3) that, at equilibrium,

$$z_{\rm E} = \frac{f_{\rm cr}(y_{\rm E})}{\omega f_{\rm br}(y_{\rm E}) + f_{\rm cr}(y_{\rm E})}.$$

Moreover,

$$\left.\frac{{\rm d}y}{{\rm d}t}\right|_{y=1} = -1 < 0.$$

Hence, if we prove that there exists a $\varepsilon > 0$ such that

$$\left.\frac{{\rm d}y}{{\rm d}t}\right|_{y=\varepsilon} > 0,$$

the intermediate value theorem ensures the existence of at least one positive (i.e., endemic) equilibrium value for y. This coincides with requiring

$$-\varepsilon + \tau\varepsilon(1-\varepsilon)\frac{f_{\rm cr}(\varepsilon)}{\omega f_{\rm br}(\varepsilon) + f_{\rm cr}(\varepsilon)} > 0.$$

Simplifying by ε on both sides and rearranging the terms, we obtain

$$\tau \frac{f_{\rm cr}(\varepsilon)}{\omega f_{\rm br}(\varepsilon) + f_{\rm cr}(\varepsilon)} > \frac{1}{1-\varepsilon}.$$

This inequality coincides with the assumption $R_0 > 1$ for $\varepsilon = 0$; hence, by continuity, there exists an $\varepsilon > 0$ such that the desired inequality is satisfied.

This concludes the proof. □

3.5 Global stability

Before proving global stability, we first consider limit cycles of the aNIMFA model, for which we invoke the Bendixson-Dulac theorem.

Theorem 3 *(Bendixson-Dulac) If there exists a C^1-function $\phi(y, z)$ such that the expression*

$$F(y,z) = \frac{\partial(\phi f)}{\partial y} + \frac{\partial(\phi g)}{\partial z} \tag{9}$$

has the same sign ($\neq 0$) almost everywhere in a simply connected region R, then the planar autonomous system

$$\frac{{\rm d}y}{{\rm d}t} = f(y,z),$$
$$\frac{{\rm d}z}{{\rm d}t} = g(y,z),$$

has no non-constant periodic solutions lying entirely within the region R.

A proof of Theorem 3 can be found in [26], or in [27] for the n-dimensional case. We now apply Theorem 3 to prove that system (3) admits no periodic solutions.

Theorem 4 *System (3) admits no non-trivial periodic solutions.*

Proof We verify the Bendixson-Dulac criterion using $\phi(y,z) = \frac{1}{yz}$ for our system (3) in the region $R = (0,1)^2$. We find

$$\phi f = -\frac{1}{z} + \tau(1-y),$$
$$\phi g = -\zeta\frac{f_{\rm br}(y)}{y} + \xi\frac{f_{\rm cr}(y)}{yz} - \xi\frac{f_{\rm cr}(y)}{y}.$$

Filling in Eq. (9) gives

$$F(y,z) = -\tau - \xi\frac{f_{\rm cr}(y)}{yz^2}.$$

Since $y, z > 0$ and $f_{\rm cr}(y)$ is a non-negative function, we conclude that $F < 0$ in the whole region $R = (0,1)^2$ and there cannot exist any limit cycles. □

Recall that the DFE is locally (hence, globally) unstable when $R_0 > 1$. We make the following remark:

Corollary 5 *Assume that $R_0 > 1$, and that the DFE is on the repelling part of the z-axis $\{y = 0, z > \frac{1}{\tau}\}$. Then, the endemic equilibrium, if it is unique, is globally asymptotically stable. If multiple endemic equilibria exist, or the DFE is in the attracting part of the z-axis, i.e. $\{y = 0, z < \frac{1}{\tau}\}$, no general conclusions can be drawn.*

Proof We can exclude the possibility of homoclinic orbits to the DFE, whose stable manifold is the z-axis. Under our assumptions, the corollary is an immediate consequence of Theorem 4. □

4 Examples

In the previous section, we derived several general results for the aNIMFA model. However, certain properties, like the number and stability of the endemic states, could not be determined for general functional responses. In this section, we investigate several examples of functional responses f_{br} and f_{cr}, whereby we primarily focus on epidemiological applications. Then, by assumption, the link-breaking rule $f_{\mathrm{br}}(y)$ is likely to be increasing with the prevalence y and the link-creation rule $f_{\mathrm{cr}}(y)$ is exactly opposite. The aNIMFA model is, however, more versatile and can be applied to other spreading phenomena, including opinion dynamics, cascading failures and information transport in the human brain. These spreading phenomena are often more complex than SIS epidemic spread, thus requiring more complex (maybe even non-monotone) functional responses f_{br} and f_{cr}.

4.1 Example 1: Random link-activation deactivation

Presumably the easiest functional responses are those that are totally unaffected by the current number of infected cases. Then the network density evolves independently of the epidemic prevalence. This model is known as the Random Link-Activation Deactivation (RLAD) model [7]. In this model, each link in the underlying network can be randomly created or broken, with rates ξ and ζ respectively. Mathematically, we require that the functional responses f_{br} and f_{cr} are constant and for simplicity, we consider $f_{\mathrm{br}}(y) = f_{\mathrm{cr}}(y) = 1$, and hence system (3) becomes

$$\frac{\mathrm{d}y}{\mathrm{d}t} = -y + \tau y(1-y)z, \tag{10a}$$

$$\frac{\mathrm{d}z}{\mathrm{d}t} = -\zeta z + \xi(1-z). \tag{10b}$$

Then, the basic reproduction number as defined in Eq. (8) is $R_0 = \frac{\tau}{1+\omega}$. In this simple example, the governing equation (3b) for the link-density $z(t)$ is decoupled from the prevalence $y(t)$ and can be solved directly;

$$z(t) = \frac{1}{1+\omega} + \left(z_0 - \frac{1}{1+\omega}\right) e^{-(\xi+\zeta)t},$$

where the effective link-breaking rate $\omega = \zeta/\xi$. If the exponential decays sufficiently fast (i.e. $\xi + \zeta$ is large), the network density quickly converges to $z = 1/(1+\omega)$. Substituting $z = 1/(1+\omega)$ into Eq. (3a) and solving yields the famous logistic equation [28] for the prevalence;

$$y(t) = \frac{y_{\mathrm{E}}}{1 + e^{-K(t-t_0)}}, \tag{11}$$

where $y_{\mathrm{E}} = 1 - \frac{1+\omega}{\tau}$ is the steady-state prevalence, $K = \tau - 1$ is the growth rate and $t_0 = \frac{1}{K} \ln\left(\frac{y_{\mathrm{E}}}{y_0} - 1\right)$ is the *inflection point*, better known as the *epidemic peak*. Formula (11) only holds if $y_0 \neq y_{\mathrm{E}}$ and the solution equals $y(t) = y_0$ if $y_0 = y_{\mathrm{E}}$.

The time-varying prevalence $y(t)$, given by Eq. (11), converges to a unique, non-zero, steady-state prevalence $y_{\mathrm{E}} > 0$ if $\tau > 1+\omega$. Otherwise, for $\tau < 1+\omega$, the prevalence decreases exponentially to zero. The same result follows from linear stability analysis. The DFE, given by $(y_{\mathrm{E}}, z_{\mathrm{E}}) = (0, \frac{1}{1+\omega})$, is asymptotically stable for $\tau < 1+\omega$, unstable for $\tau > 1+\omega$ and undetermined for $\tau = 1+\omega$. The unique endemic equilibrium is given by $(y_{\mathrm{E}}, z_{\mathrm{E}}) = \left(1 - \frac{1+\omega}{\tau}, \frac{1}{1+\omega}\right)$, which is in the biologically feasible region only if $R_0 > 1$, and coincides with the DFE when $R_0 = 1$. The Jacobian is

$$J = \begin{pmatrix} 1 - \frac{\tau}{1+\omega}\,(1+\omega)\left(1 - \frac{1+\omega}{\tau}\right) \\ 0 \qquad\qquad -\zeta - \xi \end{pmatrix}.$$

The eigenvalues are $\lambda_1 = 1 - \frac{\tau}{1+\omega}$ and $\lambda_2 = -\zeta - \xi < 0$. Thus the EE is a stable node if $R_0 > 1$, unstable node if $R_0 < 1$ and undetermined for $\tau = 1+\omega$. As we remarked above, the case $R_0 < 1$ leads to $y_{\mathrm{E}} < 0$ which is biologically infeasible. The steady states and their behavior of the RLAD model is shown in Table 1.

Since the link-dynamics is decoupled from the disease dynamics in the RLAD model, the behaviour of the RLAD model is very similar to the static SIS model and undergoes the usual transcritical bifurcation, except that the basic reproduction number R_0 is a function of the effective link-breaking rate ω. For other functional responses f_{br} and f_{cr}, we expect different behaviour, which will be investigated in the upcoming examples.

Table 1 The equilibria of Example 1 and their local stability

Example 1: $f_{br}(y) = 1$, $f_{cr}(y) = 1$	$R_0 \leq 1$	$R_0 > 1$
Disease-free state $\left(0, \frac{1}{1+\omega}\right)$	Stable node	Unstable node
Endemic equilibrium $\left(1 - \frac{1+\omega}{\tau}, \frac{1}{1+\omega}\right)$	Unstable node	Stable node

Table 2 The equilibria of Example 2 and their local stability

Example 2: $f_{\mathrm{br}}(y) = y$, $f_{\mathrm{cr}}(y) = 1$	$R_0 \leq 1$	$R_0 > 1$
Disease-free state $(0, 1)$	Stable node	Unstable node
Endemic equilibrium $\left(\frac{1-\frac{1}{\tau}}{1+\frac{\omega}{\tau}}, \frac{1+\frac{\omega}{\tau}}{1+\omega}\right)$	Unstable spiral	Stable spiral

4.2 Example 2: Epidemics: $f_{\mathrm{br}}(y) = y$, $f_{\mathrm{cr}}(y) = 1$

Contrary to the randomly evolving links in Example 1, we expect that genuine epidemic outbreaks affect the number of contacts of people. We consider the simple case where the link-breaking process $f_{\mathrm{br}}(y) = y$ is a linear function of the prevalence, but the link-creation process remains independent from the total number of infections [$f_{\mathrm{cr}}(y) = 1$]. Then, the governing equations become

$$\frac{\mathrm{d}y}{\mathrm{d}t} = -y + \tau y(1-y)z, \tag{12a}$$

$$\frac{\mathrm{d}z}{\mathrm{d}t} = -\zeta z y + \xi(1-z). \tag{12b}$$

The basic reproduction number as defined in Eq. (8) is $R_0 = \tau$. The disease-free equilibrium $(y_{\mathrm{E}}, z_{\mathrm{E}}) = (0, 1)$ is a stable node if $\tau < 1$, an unstable node if $\tau > 1$ and is otherwise undetermined. The unique EE follows from Eq. (4) as $(y_{\mathrm{E}}, z_{\mathrm{E}}) = \left(\frac{\tau-1}{\tau+\omega}, \frac{\tau+\omega}{\tau(1+\omega)}\right)$ and exists in the biologically feasible region for $\tau > 1$.

We now show that the unique EE is locally stable for this specific choice of f_{br} and f_{cr}. The Jacobian around the EE equals

$$J = \begin{pmatrix} -1 + \tau(1-2y_{\mathrm{E}})z_{\mathrm{E}} & \tau y_{\mathrm{E}}(1-y_{\mathrm{E}}) \\ -\zeta z_{\mathrm{E}} & -\zeta y_{\mathrm{E}} - \xi \end{pmatrix} = \begin{pmatrix} -\frac{\tau-1}{1+\omega} & \frac{\tau(\tau-1)(\omega+1)}{(\tau+\omega)^2} \\ -\zeta\frac{\tau+\omega}{\tau(1+\omega)} & -\zeta\frac{\tau(\omega+1)}{\omega(\tau+\omega)} \end{pmatrix}.$$

Clearly, for $\tau > 1$ and $\zeta, \omega > 0$, we have $J_{1,1}, J_{2,1}, J_{2,2} < 0$ and $J_{1,2} > 0$; hence, $\mathrm{tr}(J) < 0$ and $\det(J) > 0$, which implies that the real parts of its eigenvalues are negative. Hence, the EE is locally stable. Following Corollary 5, the EE is also globally asymptotically stable for $R_0 > 1$, which is a consequence of the absence of limit cycles guaranteed by Bendixson-Dulac and the fact that the DFE is unstable for $R_0 > 1$.

We summarize the stability of the two equilibria in Table 2 and present simulations of the two possible behaviours of system (12) in Fig. 1.

Comparing this example to Example 1, the behaviour is different in two ways. First, the basic reproduction number $R_0 = \tau$ does not depend on the link-breaking rate ζ and link-creation rate ξ. Second, the endemic equilibrium remains a globally stable equilibrium, but in this case, the endemic equilibrium shows spiral behaviour around the equilibrium.

4.3 Example 3: The Adaptive SIS model

The adaptive SIS (ASIS) model was introduced by Guo et al. [29] to describe the response of individuals to an on-going pandemic. In particular, it was assumed that links are broken between susceptible and infected nodes and (re)created between susceptible nodes. The aNIMFA approximation of the ASIS model was already analysed in [12] and the functional responses were derived as $f_{\mathrm{br}}(y) = 2y(1-y)$ and $f_{\mathrm{cr}}(y) = (1-y)^2$. The link-breaking response is similar to Example 2, but the term $1 - y$ was added to account for the fact that for large epidemic outbreaks, the susceptible population may be depleted and the possibility to break links between susceptible and infected individuals decreases, simply because of the lack of susceptible individuals. The factor 2 is a conversion factor from the original Markovian model; we keep this factor for consistency with [12]. The link-creation response is more intuitive; we expect many links to be created if the disease is almost nonexistent. Hence, we are considering

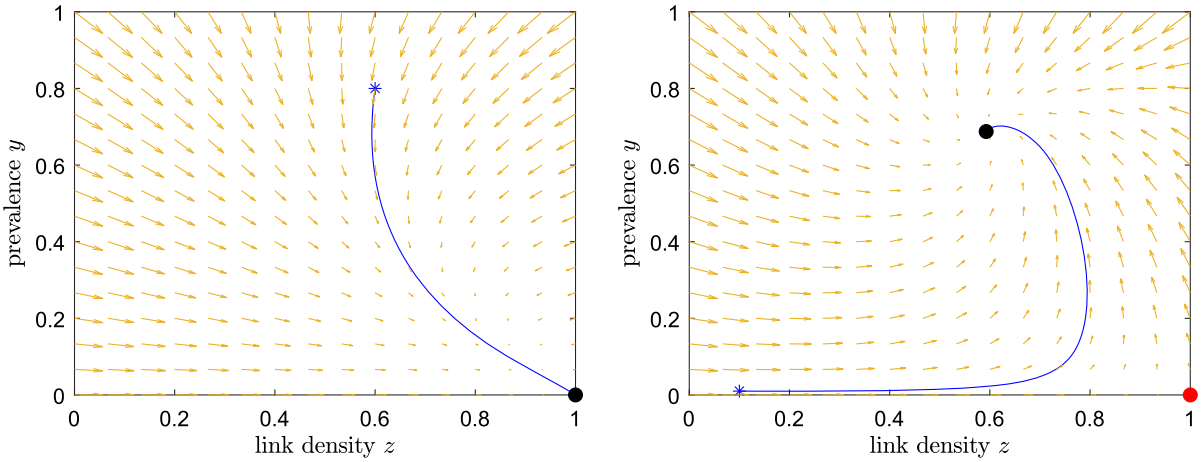

(a) $R_0 = 0.8$ (b) $R_0 = 5.4$

Fig. 1 Dynamics for Example 2. Starting point: asterisk; stable equilibrium: black dot; unstable equilibrium: red dot. **a** If $R_0 < 1$, any initial condition converges to the DFE. **b** If $R_0 > 1$, the unique EE is globally stable. The other parameters are, for simplicity, $\zeta = \xi = 1$. (Color figure online)

the system of ODEs

$$\frac{\mathrm{d}y}{\mathrm{d}t} = -y + \tau y(1-y)z, \tag{13a}$$

$$\frac{\mathrm{d}z}{\mathrm{d}t} = -2\zeta z y(1-y) + \xi(1-z)(1-y)^2. \tag{13b}$$

The basic reproduction number as defined in Eq. (8) is, once again, $R_0 = \tau$. The disease-free equilibrium $(0, 1)$ is a stable node for $R_0 < 1$, unstable node for $R_0 > 1$ and is undetermined otherwise. The unique endemic equilibrium follows from (4) and has y-coordinate [12]

$$y_\mathrm{E} = 1 - \frac{1-2\omega}{2\tau} - \sqrt{\left(\frac{1-2\omega}{2\tau}\right)^2 + \frac{2\omega}{\tau}},$$

and the EE becomes $\left(y_\mathrm{E}, \frac{1}{\tau(1-y_\mathrm{E})}\right)$. Using basic arithmetic, it can be verified that $\tau > 1$ implies $0 < y_\mathrm{E} \leq 1 - \frac{1}{\tau}$, which ensures that the EE is contained in the physical region $(0, 1)^2$. Thus, the EE exists for $R_0 > 1$.

The calculations needed for the stability of the EE become extremely cumbersome; however, the Bendixson-Dulac theorem, the uniqueness of the EE, the boundedness of solutions (see Lemma 1) and the instability of the DFE ensure that the EE is globally asymptotically stable when $R_0 > 1$ (recall Corollary 5).

Table 3 The equilibria of Example 3 and their local stability

Example 3: $f_\mathrm{br}(y) = 2y(1-y)$, $f_\mathrm{cr}(y) = (1-y)^2$	$R_0 \leq 1$	$R_0 > 1$
Disease-free state $(0, 1)$	Stable node	Unstable node
Endemic equilibrium $\left(y_\mathrm{E}, \frac{1}{\tau(1-y_\mathrm{E})}\right)$	Unstable spiral	Stable spiral

We summarize the stability of the two equilibria in Table 3 and present simulations of the two possible behaviours of system (14) in Fig. 2.

4.4 Example 4: Information spread

In this section we consider an example from opinion dynamics, where a rumour is spreading in a population. The rumour is assumed to be attractive; hence, links are created to enhance the rumour spread. We use here the Adaptive Information Diffusion (AID) model, introduced by Trajanovski et al. [30] to describe the spread of information.

The prevalence can be interpreted as the fraction of the population that knows the rumour. Infection is equivalent to hearing the news and curing corresponds to forgetting the news. As a link-breaking response, we consider $f_\mathrm{br}(y) = (1-y)^2$, which reduces the

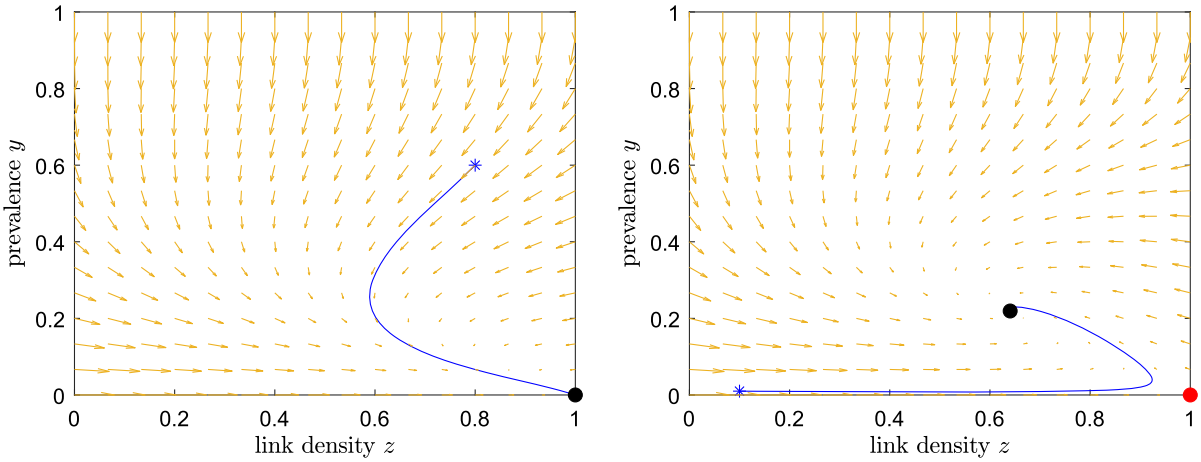

(a) $R_0 = 0.8$ (b) $R_0 = 2.0$

Fig. 2 Dynamics for Example 3. Starting point: asterisk; stable equilibrium: black dot; unstable equilibrium: red dot. **a** If $R_0 < 1$, any initial condition appears to converge to the DFE. **b** If $R_0 > 1$, the unique EE is globally stable. The other parameters are, for simplicity, $\zeta = \xi = 1$. (Color figure online)

link density when the prevalence is low. On the other hand, the link-creation response $f_{\mathrm{cr}}(y) = 2y(1-y)$ is based on the fact that the gossip is worth knowing, and thus the link density increases for larger prevalence y. However, when the news is only slightly present, little people may transmit the news to their neighbours, thereby we multiplied by the factor $(1-y)$. The factor 2 is again a conversion factor from [12]. To summarise, the system of ODEs is given by:

$$\frac{\mathrm{d}y}{\mathrm{d}t} = -y + \tau y(1-y)z, \tag{14a}$$

$$\frac{\mathrm{d}z}{\mathrm{d}t} = -\zeta z(1-y)^2 + 2\xi y(1-z)(1-y). \tag{14b}$$

The basic reproduction number R_0 cannot be determined in the traditional way using (8), as the disease-free equilibrium does not lose stability. Instead, we *define* the basic reproduction number as the point where the two endemic equilibria are born (i.e. where (16) has non-complex solutions). Then the basic reproduction number follows as [12]

$$R_0 = \frac{2\tau}{\omega + 2 + \sqrt{8\omega}}. \tag{15}$$

The disease-free equilibrium $(0,0)$ is stable for all $\tau > 0$. The y-coordinates of the two endemic equilibria follow from (4) and are equal to [12]

$$(y_{\mathrm{E}})_{1,2} = \frac{2\tau + \omega - 2 \pm \sqrt{(2\tau+\omega-2)^2 - 8\tau\omega}}{4\tau} \tag{16}$$

Table 4 The equilibria of Example 4 and their local stability

Example 4: $f_{\mathrm{br}}(y) = (1-y)^2$, $f_{\mathrm{cr}}(y) = 2y(1-y)$	$R_0 < 1$	$R_0 \geq 1$
Disease-free state $(0,0)$	Stable node	Stable node
Endemic equilibrium $\left((y_{\mathrm{E}})_1, \frac{1}{\tau(1-(y_{\mathrm{E}})_1)}\right)$	Non-existent	Unstable node
Endemic equilibrium $\left((y_{\mathrm{E}})_2, \frac{1}{\tau(1-(y_{\mathrm{E}})_2)}\right)$	Non-existent	Stable node

and the EE become $\left(y_{\mathrm{E}}, \frac{1}{\tau(1-y_{\mathrm{E}})}\right)$. The dynamics of the AID model is plotted in Fig. 3. For $R_0 < 1$, the solution converges to $(0,0)$. For $R_0 > 1$, the solution may converge to the disease-free state $(0,0)$, but also to the endemic equilibrium, depending on the initial condition. The dependence of the basic reproduction number R_0 on the effective link-breaking rate ω is nonlinear, which contrasts all earlier examples, that were either independent or linearly dependent on the effective link-breaking rate ω. Lastly, since the DFE is in the attracting part of the z-axis, we can not in general rule out the existence of a homoclinic orbit from the DFE.

We summarize the stability of the two equilibria in Table 4 and present simulations of the two possible behaviours of system (14) in Fig. 3.

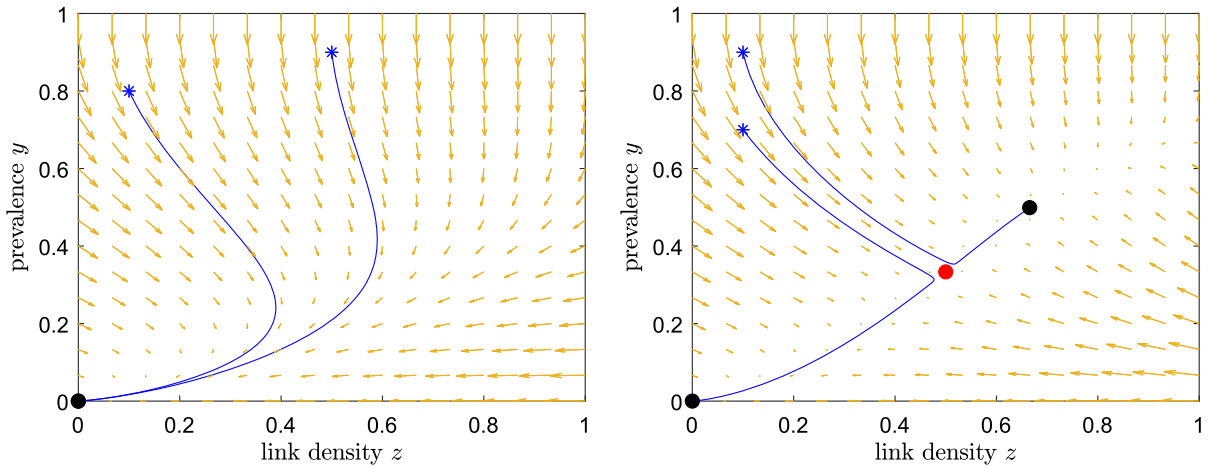

(a) $R_0 = 0.27$ (b) $R_0 = 1.03$

Fig. 3 Dynamics for Example 4. Starting points: asterisks; stable equilibrium: black dot; unstable equilibrium: red dot. (a) If $R_0 < 1$, any initial condition converges to the DFE. (b) If $R_0 > 1$, solutions may converge to the stable endemic equilibrium or the disease-free state, depending on the initial condition. The other parameters are, for simplicity, $\zeta = \xi = 1$. (Color figure online)

The basin of attraction of each stable equilibrium can be determined using a Lyapunov function. Such Lyapunov functions distinguish for which initial conditions the system will converge to either the DFE or the stable EE. However, up to the best of the authors knowledge, no exact Lyapunov function can be constructed for system (3) nor for most choices of the link-breaking and link-creation mechanisms.

However, the Lyapunov function can be approximated by considering a linearisation around a fixed point. For example, for the DFE $(0, 0)$, its Jacobian equals

$$J_{(0,0)} = \begin{pmatrix} -1 & 0 \\ 2\xi & -\zeta \end{pmatrix}.$$

According to Khalil [31, p. 73–80], we can obtain an approximate Lyapunov function $\hat{V}$ by solving for the matrix P in the following matrix equation

$$PJ + J^T P = -I,$$

and the Lyapunov function follows as

$$\hat{V}(y, z) = \begin{pmatrix} y \\ z \end{pmatrix}^T P \begin{pmatrix} y \\ z \end{pmatrix}.$$

The estimated Region of Attraction Ω is then determined by the largest $c > 0$ for which

$$\Omega_c := \{(y, z) \in [0, 1]^2 \mid \hat{V}(y, z) \leq c\},$$

is such that

$$\Omega := \max_{c>0} \left\{ \frac{\mathrm{d}}{\mathrm{d}t} \hat{V}(\Omega_c) < 0 \right\}.$$

For Example 4, the estimated Lyapunov function around $(0, 0)$ becomes

$$\hat{V}(y, z) = \frac{1}{2\zeta} z^2 + \frac{1}{2} y^2 + \frac{2\xi}{\zeta(1+\zeta)} yz + \frac{2\xi^2}{\zeta(1+\zeta)} y^2$$

which is a tedious formula, but it is clear that $\hat{V} > 0$ in the biologically relevant region $[0, 1]^2$. Unfortunately, the derivative $\frac{\mathrm{d}}{\mathrm{d}t}\hat{V}$ is extremely complicated, even in such a simple case. Hence, we derive the largest possible approximate region of attraction numerically, which is shown in Fig. 4. The approximate regions of attraction for the disease-free equilibrium $(0, 0)$ and the stable endemic equilibrium are shown in orange, whereas the exact boundary separating the two regions, and thus the actual basins of attraction of the two equilibria, is shown as a light-blue curve. The estimated regions of attraction often poorly match with the true regions of attraction [31], which is especially true for the stable EE in Fig. 4. On the other hand, the region of attraction for the DFE is reasonably accurate.

5 Slow network dynamics

Suppose now that the network dynamics in system (3) is slow compared to the disease spreading, that is to say, the disease is transmitted almost instantaneously when compared to the creation and removal of links in the network. A good example is seasonal influenza, whose

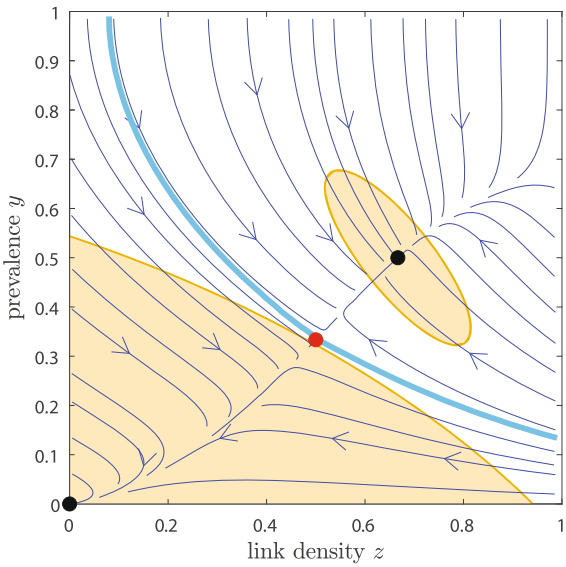

Fig. 4 Regions of attraction for Example 4. The two attraction regions are separated by the numerically determined light-blue curve, which is the stable manifold of the unstable equilibrium. The approximate regions of attraction for the disease-free equilibrium and the stable endemic equilibrium are shown in orange. Black dots denote the stable equilibria and the red dot the unstable equilibrium. The parameters are, for simplicity, $\tau = 3$, $\zeta = \xi = 1$. (Color figure online)

infection process is fast, whereas the contact network only responds very slowly to the prevalence of the disease. Analytically, this translates in the introduction of a small parameter $0 < \varepsilon \ll 1$ in the system. We perform the substitutions $\zeta \mapsto \zeta\varepsilon$ and $\xi \mapsto \varepsilon$ such that

$$\begin{aligned} \frac{\mathrm{d}y}{\mathrm{d}t} &= -y + \tau y(1-y)z, \\ \frac{\mathrm{d}z}{\mathrm{d}t} &= -\zeta\varepsilon z f_{\mathrm{br}}(y) + \varepsilon(1-z) f_{\mathrm{cr}}(y). \end{aligned} \tag{17}$$

As before, the initial conditions are $y(0) \in [0, 1]$ and $z(0) \in [0, 1]$. We assume that all parameters (including initial conditions) are $O(1)$-terms.

We intend to analyse Eq. (17) using Geometric Singular Perturbation Theory. System (17) is in standard GSPT form, and expressed in terms of the fast time variable t. In the limit $\varepsilon \to 0$, we obtain the so-called *layer equation*, or *fast subsystem*:

$$\begin{aligned} \frac{\mathrm{d}y}{\mathrm{d}t} &= -y + \tau y(1-y)z, \\ \frac{\mathrm{d}z}{\mathrm{d}t} &= 0. \end{aligned} \tag{18}$$

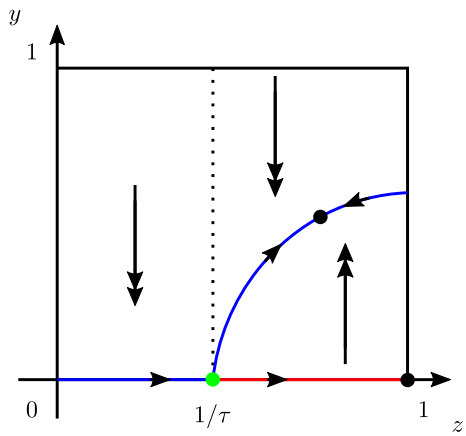

Fig. 5 Stability of the branches of the critical manifold $\mathcal{C}_0$ of (17). Blue: stable; red: unstable. Green dot: non-hyperbolic point; black dots: equilibria. Double arrows: fast flow; single arrows: slow flow. (Color figure online)

The corresponding critical manifold $\mathcal{C}_0$ is given by the union of the sets

$$\mathcal{C}_0 = \{(y, z) \in [0, 1]^2 \mid y = 0\} \cup \left\{(y, z) \in [0, 1]^2 \;\middle|\; y = \frac{\tau z - 1}{\tau z}\right\}.$$

Notice that the second branch lies in the biologically relevant quadrant of $\mathbb{R}^2$ only for $z \geq 1/\tau$, and for this branch to have a non-empty intersection with $[0, 1]^2$, we necessarily need $\tau > 1$.

Linearising the first equation of (18) and evaluating it on $y = 0$, we observe that the corresponding eigenvalue is

$$\lambda = \tau z - 1,$$

whereas the linearisation on the second branch of $\mathcal{C}_0$ gives

$$\lambda = 1 - \tau z.$$

The two branches of the critical manifold exchange stability at $(y, z) = (0, \frac{1}{\tau})$, which is a non-hyperbolic point since the linear part of system (18) is 0 here. A visualisation of the stability of the two branches of $\mathcal{C}_0$ is shown in Fig. 5.

We now rescale time, introducing the slow time variable $s = \varepsilon t$. System (17) becomes

$$\begin{aligned} \varepsilon\frac{\mathrm{d}y}{\mathrm{d}s} &= -y + \tau y(1-y)z, \\ \frac{\mathrm{d}z}{\mathrm{d}s} &= -\zeta z f_{\mathrm{br}}(y) + (1-z) f_{\mathrm{cr}}(y). \end{aligned} \tag{19}$$

Taking the limit $\varepsilon \to 0$, we obtain the so-called *reduced subsystem*. The first equation defines once again the critical manifold $\mathcal{C}_0$: substituting y in the second equation, we obtain one equation for the slow dynamics on the first branch of $\mathcal{C}_0$

$$\frac{\mathrm{d}z}{\mathrm{d}s} = -\zeta z f_{\mathrm{br}}(0) + \xi(1-z) f_{\mathrm{cr}}(0), \tag{20}$$

and one for the second

$$\frac{\mathrm{d}z}{\mathrm{d}s} = -\zeta z f_{\mathrm{br}}\left(\frac{\tau z - 1}{\tau z}\right) + \xi(1-z) f_{\mathrm{cr}}\left(\frac{\tau z - 1}{\tau z}\right). \tag{21}$$

Without further specification for the functional responses f_{br} and f_{cr}, we can hardly deduce information on the asymptotic behaviour of the system. Hence, we return to Example 2 and consider $f_{\mathrm{br}}(y) = y$ and $f_{\mathrm{cr}}(y) = 1$ such that Eqs. (20) and (21) become, respectively,

$$\frac{\mathrm{d}z}{\mathrm{d}s} = \xi(1-z),$$

and

$$\frac{\mathrm{d}z}{\mathrm{d}s} = -\zeta \frac{\tau z - 1}{\tau} + \xi(1-z). \tag{22}$$

The corresponding steady-states are $z_0 = 1$, representing the DFE, which the system tends towards if $y(0) = 0$, and

$$z_{\mathrm{E}} = \frac{\omega + \tau}{\tau\omega + \tau} \in \left(\frac{1}{\tau}, 1\right), \qquad \text{if } \tau > 1, \tag{23}$$

representing the EE, which is globally asymptotically stable for orbits on the second branch of $\mathcal{C}_0$. Given that $\tau > 1$ and further assuming that $y(0) > 0$, two difference kinds of behaviour exist.

If $z(0) < 1/\tau$, the system quickly approaches the line $y = 0$, where z starts to increase. We observe a delayed loss of stability, and we can approximate the dynamics in a neighbourhood of $y = 0$ with the so-called entry-exit function [32–34]. We remark that an orbit may not "follow" the stable branches directly, but can instead remain in the vicinity of the unstable manifold [35]. An orbit entering a neighbourhood of $y = 0$ at a point with z-coordinate $z = z_{\mathrm{in}}$ will exit the same neighbourhood at a point with z-coordinate $z = z_{\mathrm{out}} > 1/\tau > z_{\mathrm{in}}$. The value z_{out} is given implicitly as the unique solution of

$$\int_{z_{\mathrm{in}}}^{z_{\mathrm{out}}} \frac{\tau z - 1}{1 - z} \mathrm{d}z = 0.$$

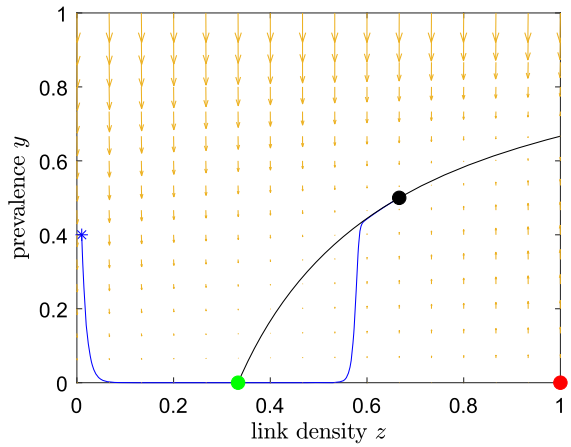

Fig. 6 The entry-exit behaviour of the fast-slow system (17) for Example 2. Parameters are $R_0 = \tau = 3, \xi = \zeta = 1, \varepsilon = 0.01$. The blue trajectory starts at the asterisk, exhibits a slow passage close to $y = 0$ and then converges to the stable EE, indicated by the black dot. The red dot is the unstable equilibrium and the green dot is the non-hyperbolic fixed point. The solid black line represents the branch of the critical manifold characterized by $y > 0$. (Color figure online)

Since the integrand function diverges at $+\infty$ as $z \to 1$, it follows that the exit point z_{out} will be strictly smaller than 1 for any $z(0) \in [0, 1/\tau)$. We refer to [17, Sec. 3] for a detailed analysis of a similar entry-exit function, derived from a different epidemiological model.

If $z(0) > 1/\tau$, the fast dynamics brings the system close to the second branch of $\mathcal{C}_0$; once an orbit reaches an $\mathcal{O}(\varepsilon)$ neighbourhood of this curve, the slow dynamics tends asymptotically towards z_{E}.

To summarize, if $y(0) = 0$, the system tends towards the equilibrium $(y, z) = (0, 1)$. If instead $y(0) \in (0, 1]$, the system converges, possibly after a slow passage near $y = 0$ which represents a "dormant" phase for the infection, towards the endemic equilibrium

$$(y_{\mathrm{E}}, z_{\mathrm{E}}) = \left(\frac{\tau - 1}{\omega + \tau}, \frac{\omega + \tau}{\tau\omega + \tau}\right) \in (0, 1]^2.$$

We emphasise that this holds true only for $R_0 = \tau > 1$. Figure 6 provides a numerical simulation that shows the entry-exit phenomenon.

6 Conclusion

In this paper, we developed a minimal model for modelling an SIS disease spread with personal contact avoidance, called adaptive NIMFA (aNIMFA). We

investigated local and global stability of the model and showed that limit cycles cannot exist. The non-existence of limit cycles implies that epidemic waves cannot occur in this SIS model based on disease and behaviour dynamics alone and time-varying parameters are required to exhibit epidemic waves. Furthermore, we analysed various examples in detail, from epidemic contagion to information spread.

In this work, we assumed an homogeneous mixing of the population. In reality, this homogeneity is often unrealistic; some people have frequent contacts while other people never meet. We expect that one can extend the current results for a community of subpopulations, on a network with N nodes, as it was done in [36] in order to generalize the results obtained in [37] for SAIRS compartmental models. While considering subpopulations, one must decide whether the link-breaking and link-creation functional responses act on the local prevalence of the node or on the global prevalence of the whole network. From a modelling perspective, we see possibilities for both approaches, or a mix of these [38].

We see several other interesting directions for future research. For example, is it possible to provide, besides continuity, conditions on f_{br} and f_{cr} such that we can limit/bound the number of endemic equilibria from Eq. (4)? Can we determine for which f_{br} and f_{cr} the endemic equilibrium is unique?

Moreover, for other types of infectious diseases, it could be beneficial to consider the opposite slow-fast decomposition, compared to the one we analysed in Sect. 5. Namely, one could consider the network dynamics to be much faster than the spread of the disease, possibly including an Exposed or Asymptomatic compartment through which Susceptible individuals need to pass before becoming Infected and infectious. As a final comment, we mention the possibility to include delays into the knowledge about the current prevalence. As the COVID-19 pandemic exemplified, testing an individual typically takes several hours or days before the result is communicated. Moreover, the daily reported cases by governmental agencies typically run a few days behind. One modelling approach is to convert the aNIMFA model into a delay-differential equation, which typically complicates the analysis significantly. We leave these possibilities as an outlook for future works.

Author contributions Both authors contributed to the conceptual foundation of the manuscript. Both authors derived the mathematical results. MA worked out the examples. MS performed the GSPT analysis. MA wrote the first draft. MS commented on the draft and revised the manuscript. All authors read and approved the final manuscript.

Funding The authors declare that no funds, grants, or other support were received during the preparation of this manuscript.

Data availability The datasets generated during and/or analysed during the current study are available from the corresponding authors on reasonable request.

Declarations

Conflict of interest The authors have no relevant financial or non-financial interests to disclose.

Ethical approval Not applicable.

Consent to participate Not applicable.

Consent for publication Not applicable.

Code availability Not applicable.

References

1. Salathdé, M., Kazandjieva, M., Lee, J.W., Levis, P., Feldman, M.W., Jones, J.H.: A high-resolution human contact network for infectious disease transmission. Proc. Nat. Acad. Sci. **107**(51), 22020–22025 (2010). https://doi.org/10.1073/pnas.1009094108
2. Pastor-Satorras, R., Castellano, C., Van Mieghem, P., Vespignani, A.: Epidemic processes in complex networks. Rev. Mod. Phys. **87**, 925–979 (2015). https://doi.org/10.1103/RevModPhys.87.925
3. Gross, T., Blasius, B.: Adaptive coevolutionary networks: a review. J. Royal Soc. Interface **5**(20), 259–271 (2008). https://doi.org/10.1098/rsif.2007.1229
4. Verelst, F., Willem, L., Beutels, P.: Behavioural change models for infectious disease transmission: a systematic review (2010–2015). J. Royal Soc. Interface **13**(125), 20160820 (2016). https://doi.org/10.1098/rsif.2016.0820
5. Sahneh, F.D., Vajdi, A., Melander, J., Scoglio, C.M.: Contact adaption during epidemics: a multilayer network formu-

lation approach. IEEE Trans. Netw. Sci. Eng. **6**(1), 16–30 (2019). https://doi.org/10.1109/TNSE.2017.2770091
6. Gross, T., D'Lima, C.J.D., Blasius, B.: Epidemic dynamics on an adaptive network. Phys. Rev. Lett. **96**, 208701 (2006). https://doi.org/10.1103/PhysRevLett.96.208701
7. Kiss, I.Z., Berthouze, L., Taylor, T.J., Simon, P.L.: Modelling approaches for simple dynamic networks and applications to disease transmission models. Proc. R. Soc. A **468**, 1332–1355 (2012). https://doi.org/10.1098/rspa.2011.0349
8. Achterberg, M.A., Dubbeldam, J.L.A., Stam, C.J., Van Mieghem, P.: Classification of link-breaking and link-creation updating rules in susceptible-infected-susceptible epidemics on adaptive networks. Phys. Rev. E **101**, 052302 (2020). https://doi.org/10.1103/PhysRevE.101.052302
9. Jolad, S., Liu, W., Schmittmann, B., Zia, R.K.P.: Epidemic spreading on preferred degree adaptive networks. PLOS ONE **7**(11), 1–11 (2012). https://doi.org/10.1371/journal.pone.0048686
10. Brauer, F.: A simple model for behaviour change in epidemics. BMC Public Health **11**(1), 1–5 (2011). https://doi.org/10.1186/1471-2458-11-S1-S3
11. Van Mieghem, P.: The N-intertwined SIS epidemic network model. Computing **93**, 147–169 (2011). https://doi.org/10.1007/s00607-011-0155-y
12. Achterberg, M.A., Van Mieghem, P.: Moment closure approximations of susceptible-infected-susceptible epidemics on adaptive networks. Phys. Rev. E **106**, 014308 (2022). https://doi.org/10.1103/PhysRevE.106.014308
13. Holling, C.S.: The Components of Predation as Revealed by a Study of Small-Mammal Predation of the European Pine Sawfly. The Canadian Entomologist **91**(5), 293–320 (1959). https://doi.org/10.4039/Ent91293-5
14. Fenichel, N.: Geometric singular perturbation theory for ordinary differential equations. J. Diff. Eq. **31**(1), 53–98 (1979)
15. Kuehn, C.: Multiple Time Scale Dynamics, vol. 191. Springer, Switzerland (2015)
16. Jardón-Kojakhmetov, H., Kuehn, C., Pugliese, A., Sensi, M.: A geometric analysis of the SIR, SIRS and SIRWS epidemiological models. Nonlin. Anal. Real World Appl. **58**, 103220 (2021). https://doi.org/10.1016/j.nonrwa.2020.103220
17. Jardón-Kojakhmetov, H., Kuehn, C., Pugliese, A., Sensi, M.: A geometric analysis of the SIRS epidemiological model on a homogeneous network. J. Math. Biol. **83**(4), 1–38 (2021)
18. Brauer, F.: A singular perturbation approach to epidemics of vector-transmitted diseases. Infect. Dis. Model. **4**, 115–123 (2019)
19. Bravo de la Parra, R., Sanz-Lorenzo, L.: Discrete epidemic models with two time scales. Adv. Diff. Eq. 2021(1), 1–24 (2021)
20. Schecter, S.: Geometric singular perturbation theory analysis of an epidemic model with spontaneous human behavioral change. J. Math. Biol. **82**(6), 1–26 (2021)
21. Zhang, Z., Suo, Y., Peng, J., Lin, W.: Singular perturbation approach to stability of a SIRS epidemic system. Nonlin. Anal. Real World Appl. **10**(5), 2688–2699 (2009)
22. Aguiar, M., Kooi, B., Pugliese, A., Sensi, M., Stollenwerk, N.: Time scale separation in the vector borne disease model SIRUV via center manifold analysis. medRxiv (2021)
23. Diekmann, O., Heesterbeek, J.A.P., Metz, J.A.J.: On the definition and the computation of the basic reproduction ratio R 0 in models for infectious diseases in heterogeneous populations. J. Math. Biol. **28**(4), 365–382 (1990)
24. Driessche, P.v.d., Watmough, J.: Reproduction numbers and sub-threshold endemic equilibria for compartmental models of disease transmission. Math. Biosci. 180(1), 29–48 (2002). 10.1016/S0025-5564(02)00108-6
25. Diekmann, O., Heesterbeek, J.A.P., Roberts, M.G.: The construction of next-generation matrices for compartmental epidemic models. J. Royal Soc. interface **7**(47), 873–885 (2010)
26. Bendixson, I.: Sur les courbes définies par des équations différentielles. Acta Math. **24**, 1–88 (1901)
27. Li, Y., Muldowney, J.S.: On Bendixson's criterion. J. Diff. Eq. **106**(1), 27–39 (1993)
28. Verhulst, P.F.: Recherches mathématiques sur la loi d'accroissement de la population, 1–45 (1845)
29. Guo, D., Trajanovski, S., van de Bovenkamp, R., Wang, H., Van Mieghem, P.: Epidemic threshold and topological structure of susceptible-infectious-susceptible epidemics in adaptive networks. Phys. Rev. E **88**, 042802 (2013). https://doi.org/10.1103/PhysRevE.88.042802
30. Trajanovski, S., Guo, D., Van Mieghem, P.: From epidemics to information propagation: Striking differences in structurally similar adaptive network models. Phys. Rev. E **92**, 030801 (2015). https://doi.org/10.1103/PhysRevE.92.030801
31. Khalil, H.K.: Nonlinear Control, global Pearson Education, Essex, England (2015)
32. De Maesschalck, P., Schecter, S.: The entry-exit function and geometric singular perturbation theory. J. Diff. Eq. **260**(8), 6697–6715 (2016)
33. Neishtadt, A.I.: Persistence of stability loss for dynamical bifurcations I. Diff. Eq. **23**, 1385–1391 (1987)
34. Neishtadt, A.I.: Persistence of stability loss for dynamical bifurcations II. Diff. Eq. **24**, 171–176 (1988)
35. Krupa, M., Szmolyan, P.: Extending slow manifolds near transcritical and pitchfork singularities. Nonlinearity **14**(6), 1473 (2001)
36. Ottaviano, S., Sensi, M., Sottile, S.: Global stability of multi-group SAIRS epidemic models. arXiv preprint arXiv:2202.02993 (2022)
37. Ottaviano, S., Sensi, M., Sottile, S.: Global stability of SAIRS epidemic models. Nonlin. Anal. Real World Appl. **65**, 103501 (2022)
38. Zhang, L., Guo, C., Feng, M.: Effect of local and global information on the dynamical interplay between awareness and epidemic transmission in multiplex networks. Chaos: An Interdisciplinary J. Nonlin. Sci. 32(8), 083138 (2022). 10.1063/5.0092464